

2018

# Evaluating the Impact of the Measurement Setup on Cyclic Degradation Coefficient of Air Conditioning Systems

Rohit Dhumane

*University of Maryland, United States of America, dhumane@umd.edu*

Tianyue Qiu

*Center for Environmental Energy Engineering, University of Maryland, College Park, 4164 Glenn Martin Hall, MD 20742, USA, tyqiu@umd.edu*

Jiazhen Ling

*University of Maryland, College Park, United States of America, jiazhen@umd.edu*

Vikrant Chandramohan Aute

*University of Maryland College Park, vikrant@umd.edu*

Yunho Hwang

*yhhwang@umd.edu*

*See next page for additional authors*

Follow this and additional works at: <https://docs.lib.purdue.edu/iracc>

---

Dhumane, Rohit; Qiu, Tianyue; Ling, Jiazhen; Aute, Vikrant Chandramohan; Hwang, Yunho; Radermacher, Reinhard; Kirkwood, Allen Chad; and Esformes, Jack, "Evaluating the Impact of the Measurement Setup on Cyclic Degradation Coefficient of Air Conditioning Systems" (2018). *International Refrigeration and Air Conditioning Conference*. Paper 2012. <https://docs.lib.purdue.edu/iracc/2012>

This document has been made available through Purdue e-Pubs, a service of the Purdue University Libraries. Please contact [epubs@purdue.edu](mailto:epubs@purdue.edu) for additional information.

Complete proceedings may be acquired in print and on CD-ROM directly from the Ray W. Herrick Laboratories at <https://engineering.purdue.edu/Herrick/Events/orderlit.html>

---

**Authors**

Rohit Dhumane, Tianyue Qiu, Jiazhen Ling, Vikrant Chandramohan Aute, Yunho Hwang, Reinhard Radermacher, Allen Chad Kirkwood, and Jack Esformes

## Evaluating the Impact of the Measurement Setup on Cyclic Degradation Coefficient of Air Conditioning Systems

Rohit DHUMANE<sup>1</sup>, Tianyue QIU<sup>1</sup>, Jiazhen LING<sup>1</sup>, Vikrant AUTE<sup>1\*</sup>, Yunho HWANG<sup>1</sup>, Reinhard RADERMACHER<sup>1</sup>, Allen Chad KIRKWOOD<sup>2</sup>, Jack ESFORMES<sup>3</sup>

<sup>1</sup>Center for Environmental Energy Engineering, 4298 Campus Dr., 4164A Glenn Martin Hall, University of Maryland, College Park, MD, USA 20742

Phone: 301-405-7661, Email: {dhumane, tyqiu, jiazhen, vikrant, yhhwang, raderm}@umd.edu

<sup>2</sup>Carrier Corporation,  
7310 West Morris Street, Indianapolis, IN, USA 46231  
Email: allenchad.kirkwood@carrier.utc.com

<sup>3</sup>Carrier Corporation,  
6304 Carrier Parkway, TR19 Syracuse, NY, USA 13221  
Email: Jack.Esformes@carrier.utc.com

\* Corresponding Author

### ABSTRACT

Building Heating, Ventilation and Air Conditioning (HVAC) is one of the largest primary energy consumers in the United States. Vapor Compression Systems (VCS), which are at the heart of building HVAC, are typically sized for peak operation, but operate at part load most of the time. The current rating standards are conceived to provide credit to designs that have higher efficiency in the part load operation. However, the current evaluation procedure is not sufficiently standardized; the same system could be tested in different test facilities and yield different performance results. These deviations arise from such factors including, but not limited to, test setup (called code tester) thermal inertia, length and orientation of suction line and vapor line that affects refrigerant migration during off cycle, and frequency of operation of dampers to regulate airflow in code testers. These are not captured in the current procedure. The current article aims at quantification of the thermal inertia effects of the code tester and its impact on the evaluation of cyclic degradation coefficient ( $C_d$ ) in a split air conditioning system. A new term called “thermal inertia factor” (TIF) is added to the formulation of the  $C_d$  to account for the code tester thermal inertia. A conventional residential split air conditioning system is tested in two different code testers to obtain two different values of the  $C_d$ . A physically based model of code tester is developed using Modelica and validated with experimental data. TIF’s for both code testers are evaluated using this model. The new equation is able to predict the  $C_d$  obtained in the second setup from the first setup experimental results and the TIF of the second experimental setup. The current study is the first of its kind and is expected to improve existing test procedures by removing variations arising from differences in code tester designs at various laboratories. Parametric studies on air flow rates and code tester system temperatures are carried out to quantify the TIF and understand the effect of various factors on it.

**Keywords:** HVAC, Cyclic degradation, Rating standards, Code Tester

### 1. INTRODUCTION

Building HVAC is sized for peak load conditions, meaning that the system is oversized for most of its operation. Due to this, a typical operation of conventional air conditioners involves alternating on-off cycling, which is a major contributor to performance degradation. The part load cyclic performance needs to be captured to estimate annual heat pump energy consumption and operational cost. This was the motivation for the Department of Energy (DOE) when it introduced new regulations that introduced seasonal energy efficiency ratio (SEER) in 1979 (Didion and Kelly, 1979). A similar procedure was adopted by the American Society of Heating, Refrigerating, and Air-Conditioning Engineers (ASHRAE) in 1983, which is still continued with the latest errata released in 2010 (ASHRAE Standard 116, 2010). The objective of these standards is to provide fair credit to more efficient products. However, the standards

were developed roughly four decades ago when computational resources were limited and research regarding the complexities of HVAC system cyclic operation was sparse. At present, the availability of vastly superior computational resources coupled with the existence of excellent frameworks for modeling complex systems and a rich knowledge from numerous experiments conducted over the years, provides several opportunities for improvement of these standards.

The present article starts by briefly reviewing the existent rating procedure to highlight a few areas for potential improvements. The motivation for the present article is to reduce the variation in the measured value of the cyclic degradation coefficient ( $C_d$ ) for the same system from two different airflow measurement equipment (called code testers). The research effort is focused towards analyzing and then mitigating these variations. Validated dynamic models using Modelica (Mattsson et al., 1998) are used to investigate the behavior of code testers. Finally, a new parameter is introduced, which shows the potential of removing the impact of code tester from the  $C_d$  measurements. An example calculation based on experimental data is discussed to show the applicability of the suggested procedure. The article is the first effort of its kind towards the improvement of the rating standards, which apply to the devices that are one of the highest contributors to a country's primary energy consumption.

## 2. CODE TESTER

Code testers are described in ASHRAE Standard 41.2 (1992), which provides recommended practices for airflow measurements. The test chamber is a generic name applied to these devices, but code tester has also been used for many years. The code tester (the airflow measuring apparatus in Figure 1) consists of ducts for airflow passage from the test unit with pressure and temperature being measured at various locations along the passage. Flow settling devices (mixers) are placed in portions of the air duct to reduce the temperature gradient in the airflow. Nozzles, along with calibration correlations, are used to determine the air volume flow rate. A few dimensional constraints are applicable to their geometry. However, due to a wide variety of possibilities from these constraints, the code tester designs at different facilities are likely quite different. There are also no guidelines on material selection for code tester fabrication. These aspects lead to significant variations in the thermal inertia effects for a tested unit in different code testers.

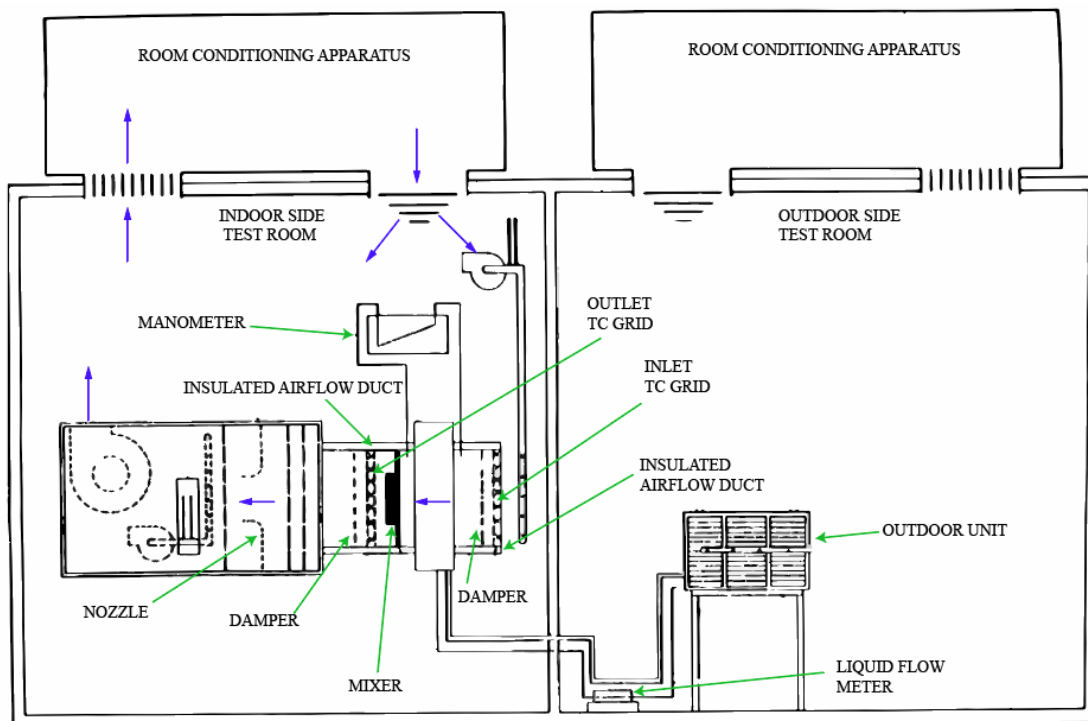


**Figure 1:** Tunnel Air Enthalpy Method Arrangement (redrawn from ASHRAE Standard 116, 2010)

Split air conditioners (SPAC) are tested using separate environmental chambers for both an indoor unit (IDU) and outdoor unit (ODU) as shown in Figure 1. The method used for calculating the net cooling capacity of SPAC is called the tunnel air enthalpy test. The code tester needs to be connected to only the IDU for the case of SPAC. A room conditioning apparatus maintains the IDU chamber to a fixed temperature, which is measured by the inlet thermocouple grid. The air flows over the IDU, where it gets cooled if the SPAC is ON. The code tester includes a mixer, an outlet thermocouple grid, nozzles and dampers, all of which are enclosed within an insulated duct. An exhaust fan drives the air to the room conditioning apparatus to be reconditioned to the IDU chamber temperature.

Due to space constraints, the different portions of the code tester may all not be in the same horizontal plane and/or along the same horizontal axis. The insulated airflow duct shown in Figure 1 may consist of multiple ducts of varying lengths and bends. The whole setup is confined to a single room. However, to avoid entrance flow effects and temperature gradients from bends, the airflow length may be as large as 8-15 meters. Such a code tester has significant thermal inertia which should be accounted for in the data reduction.

### 3. CURRENT EVALUATION PROCEDURE

The DOE and ASHRAE standards for evaluation of part load performance are based on the experimental work of Kelly and Parken (1978) conducted at National Institute of Standards and Technology (then called National Bureau of Standards). Parken et al. (1977) introduced the non-dimensional forms of efficiency (called part load factor, PLF) and cyclic cooling capacity (called cooling load factor, CLF) as per Equations (1) and (2). The PLF and CLF were related by a linear fit even though there were variations in the PLF data due to the cycling rate. This led to the development of the degradation coefficient,  $C_d$ , as defined by Equation (3). The part load factor in Equation (4) [PLF (0.5)] is evaluated for a CLF of 0.5 to estimate the SEER.

$$PLF = \left( \frac{COP_{cyc,dry}}{COP_{ss,dry}} \right) \quad (1)$$

$$CLF = \left( \frac{\int_0^{t_o} \dot{Q}_{cyc,dry} dt}{\dot{Q}_{ss,dry} t_c} \right) \quad (2)$$

$$C_d = \frac{1 - PLF}{1 - CLF} \quad (3)$$

$$SEER = [PLF(0.5)][EER_b] \quad (4)$$

This SEER evaluation procedure is based on experimental data available at that time without any significant theoretical research. Starting from Murphy and Goldschmidt (1979), Goldschmidt et al. (1980) to O'Neal and Katipamula (1993), in efforts spanning well over a decade, several researchers conducted extensive experimental and theoretical investigations to understand the validity of the assumptions made in the development of the procedure.

Single time constant models, which model start-up cooling capacity of the air conditioner as an exponential function of the time constant, were used by Katipamula and O'Neal (1991), and O'Neal and Katipamula (1993) to show that the relationship between PLF and CLF is not linear. Henderson et al. (2000) found that the use of  $C_d$  to evaluate PLF (by simple substitution in Equation (3)) is not accurate and implemented alternate empirical equation in DOE-2, a building energy simulation program. Experiments conducted by Bettanini et al. (2003) to evaluate the use of  $C_d$  to evaluate PLF from Equation (3), show that this approximation is not acceptable. They propose a new parameter  $Z$ , which is the ratio of the electric power consumption at the part load working condition to that at full capacity to evaluate PLF. Italian standard UNI 10963 also identifies the shortcoming of  $C_d$  and uses the  $Z$ -parameter method to evaluate PLF (Bettanini et al., 2003). However, the ISO Standard 16358-1 (2013) still uses  $C_d$  and defines 0.25 as the default value.

The single-time-constant model assumes that the shutdown transients have no direct impact on the startup characteristics. The startup losses can be better predicted by two-time-constant models (Mulroy and Didion, 1985), with one time constant capturing the capacity delay due to the mass of the heat exchanger, while the second time constant capturing the delay in reaching steady state refrigerant distribution from the off-cycle refrigerant distribution. Sigmoid and polynomial functions for startup have been used by Fuentes et al. (2016). However, the behavior of PLF and CLF obtained by integrating these functions has not been investigated.

The heat losses to the test setup have not been considered by any of these researchers. AHRI Standard 210/240 (2017) as well as ASHRAE Standard 116 (2010) recognize the contribution of the code tester in the measured cyclic cooling capacity by introducing a correction procedure. For the discussion of the present article, since the focus is on air-conditioners, we will focus only on the indoor room apparatus in laboratory testing of split air conditioners. The method is described in the operation manual of AHRI Standard 210/240 (2017) and is summarized here. An electric heater is used as the source for integrated measured capacity and is cycled every 6 minutes with alternating on and off cycles. Ten on-off cycles are carried out over a two-hour duration with a fixed airflow of  $0.566 \text{ m}^3\text{s}^{-1}$  (1200 cfm). The temperature at the location of highest thermal mass (typically, the mixer) is measured at the start and end of the off cycle. For the discussion in this section, it will be assumed that this assumption is valid.

The average value of integrated airside capacity ( $q_{ts,avg}$ ) evaluated as per ASHRAE Standard 116 (2010) from last 6 to 8 cycles of the 10 on-off cycles is calculated using Equation (5). The integrated capacity ( $q'$ ) is corrected using the thermal inertia term calculated from Equation (5) as shown in Equation (6). The temperature difference at the beginning and end of the off cycle is used in Equation (5) while that during the on time during the cyclic D-Test AHRI Standard 210/240 (2017) for the mixer in Equation (7). The dampers that circulate air into the code tester may have a different cycling time than the compressor and in such cases, the integration time should be taken from damper cycling. However, this is much closer to the on-cycle time in D-Test and so it is assumed equal in Equation (7).

$$q_{ts,avg} = \overline{m\dot{c}} \frac{(\Delta T_1)_{off,mixer}}{t_{off}} \quad (5)$$

$$q = q' + \overline{m\dot{c}} (\Delta T_1)_{on,mixer} \quad (6)$$

$$q_{ts} = \int_{off} \dot{Q}.dt = \sum_{i=1}^n m_i c_i (\Delta T_i)_{off} \quad (7)$$

$$\overline{m\dot{c}} = m_1 c_1 + \left( \sum_{i=2}^n m_i c_i \frac{(\Delta T_i)_{off}}{(\Delta T_1)_{off}} \right) \quad (8)$$

In the real case, the  $q_{ts}$  term should involve heat transfer from all the regions of the code tester. If the code tester has “n” different regions indexed along the decreasing order of their thermal inertia, the mixer will get index of 1 with the assumption of it being the region of highest thermal inertia. Now, the thermal inertia term evaluated in Equation (5) is given by Equation (8). Therefore, the standard ignores the second term on the right-hand side of Equation (8). It has been observed that this assumption leads to underprediction of thermal inertia effects from a code tester (by as much as 70% as will be shown later), and is one of the reasons for the differences in measured values of  $C_d$  for the same system when tested with different code testers.

#### 4. THERMAL INERTIA EFFECTS IN CODE TESTER

The present study evaluates two code testers with significantly different thermal inertia. One has a very high thermal inertia due to longer duct passage and higher amount of material, while the other is designed to keep the thermal inertia at a minimum. The higher thermal inertia code tester will be referred to as CT-A, while the one with lower thermal inertia will be referred to as CT-B. The exact geometry of these code testers is proprietary and therefore not presented herein. However, the equations and calculation methods are discussed in such a manner that it may be applied to any design for a reader interested in conducting a similar analysis.

The product of mass and specific heat capacity of materials at different regions along airflow direction for CT-A are plotted in Figure 2. An airflow duct is made up of three layers: inner and outer steel plates with insulation foam in between. Only the regions between the two thermocouple grids (see Figure 1) is included because the region after the second TC grid does not influence the measured temperature difference used for evaluating capacity. We can observe that the thermal mass is very well distributed throughout the code tester and there is no region which may be used as the dominating thermal inertia effect (say >90%) region mentioned in the standard. The mixer has one of the smallest thermal inertia, but it lies entirely along the airflow passage and will capture much more heat than a duct.

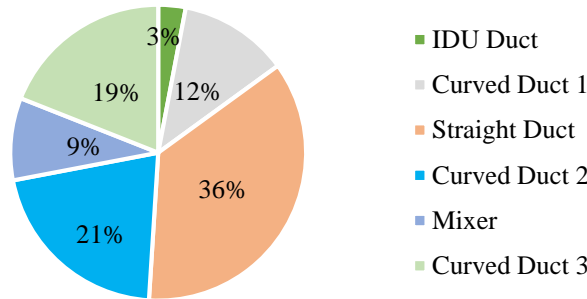


Figure 2: Distribution of thermal inertia of CT-A

To capture the dynamic response of various regions of the code tester, a model (Figure 3a) is constructed using components from the *Modelica Standard Library* (Modelica Association, 2008) and *Buildings Library* (Wetter et al., 2014). The connections for heat transfer are shown in red (HeatPort), while the connections in blue are fluid flow connections (FluidPort). The ThermalConductor block models transport of heat without storing it and needs the input of thermal resistance Equation (9). Churchill & Chu (1975) correlation is used to evaluate heat transfer coefficients for natural convection from the outer surface of airflow duct to the environment chamber. This is then multiplied by the area and provided as an input. The HeatCapacitor block (Equation (10)) is a generic model for the heat capacity of the material. The thermal inertia (C) is provided as input parameter and used to update temperature (T) of the block based on the rate of heat transfer.

The model used for straight duct is shown in Figure 3b. It contains a Mixed Volume block (Buildings.Fluid.MixingVolumes.MixingVolume) and Fixed Flow Resistance block (Buildings.Fluid.FixedResistances.PressureDrop) from the Buildings Library to model the airflow.

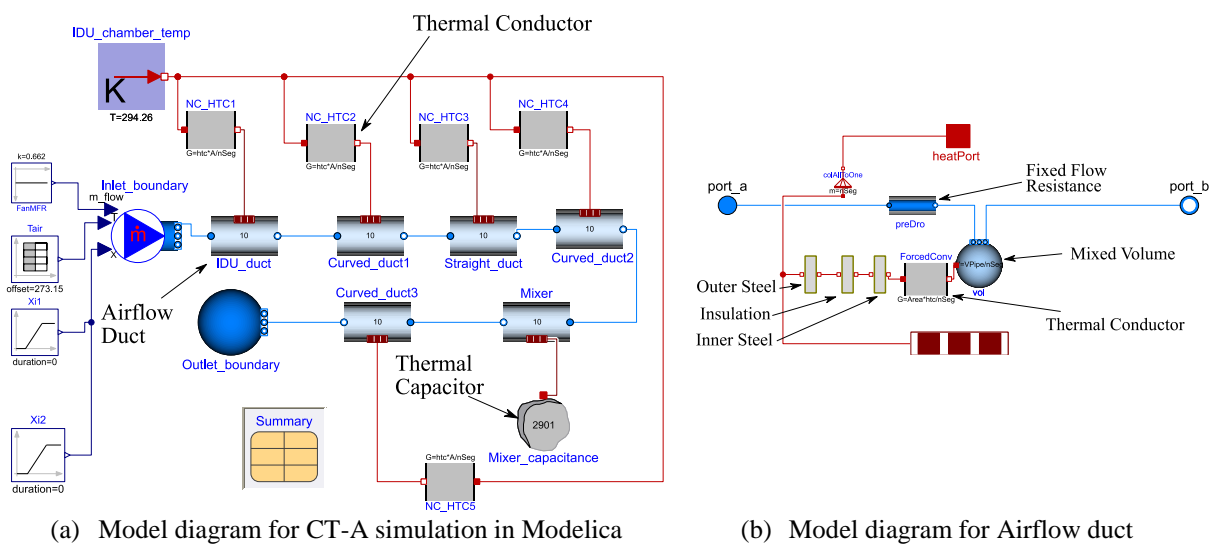
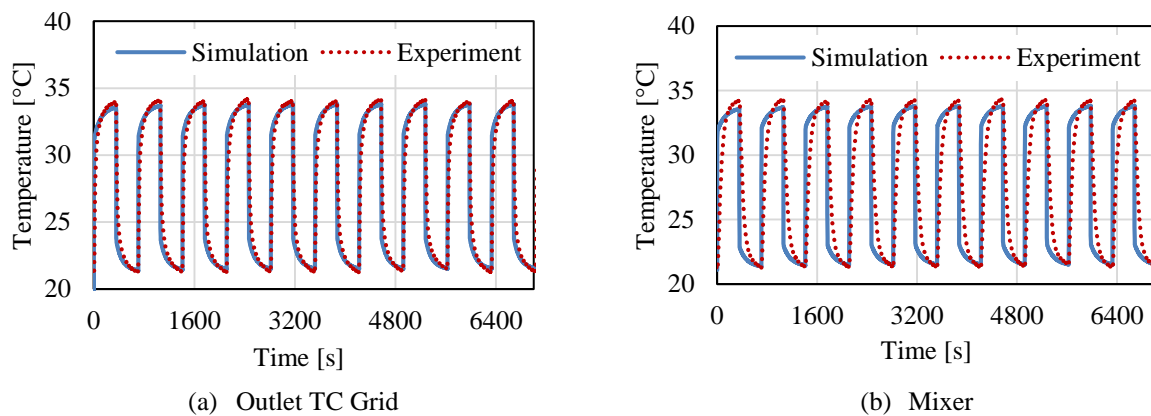


Figure 3: Modelica model details

$$\dot{Q} = G(\Delta T) \quad (9)$$

$$mc \frac{dT}{dt} = \dot{Q} \quad (10)$$

The Mixed Volume block models the air as instantaneously mixed in the segment of the duct. The mixed volume is connected to three TubeWall blocks, each of which represents the three layers of the duct (inner steel sheet, insulation foam and the outer steel sheet). The TubeWall block is a simplified version of Modelica.Fluid.Examples.HeatExchanger.BaseClasses.WallConstProps and is a pipe wall with capacitance assuming 1D heat conduction with constant material properties. A ThermalConductor block is used to model the heat transfer resistance between the airside and the inner steel sheet. Dittus & Boelter (1985) correlation is used to calculate the internal forced flow heat transfer coefficient. The flow resistance block contains a quadratic relation between mass flow rate and pressure drop, with nominal values required as inputs. A similar composition of blocks is used to model different locations, the only difference being the surface area and heat transfer coefficient inputs provided as parameters. The heat transfer coefficient enhancement in bends is also accounted for using Schmidt (1967) correlation. The cyclic heater behavior is simulated by providing a square profile for temperature as a function of time as input using a TimeTable block. During the off cycle, the temperature equals the room temperature and during the on cycle, it equals the temperature corresponding to the temperature available for sensible heat increase of the air stream corresponding to the heater capacity.



**Figure 4:** Validation of the code tester model with experiment data

The model is run with the Radau-IIa solver with a tolerance of  $10^{-6}$  and is validated with temperature readings available at the outlet thermocouple grid and mixer location from the heater test for CT-A (see Figure 4). The model shows a good match with trends from experimental data and can be used to investigate the behavior of the code tester. The heat stored in different regions of the code tester can be evaluated by integrating the capacity measured across the inlet and outlet of individual components from the model. The results are plotted in Figure 5. These percentages are much different from the plot of thermal inertia (Figure 2). One of the main reasons for the deviation is that the steel plate on the outside, having large thermal inertia does not contribute to the cyclic heat transfer. The mixer does indeed store the highest amount of heat in the code tester, but it is by no means a dominating contribution (>90%). As described earlier (Equation (7)), the code tester correction will be much smaller (29% of the actual) as per (AHRI Standard 210/240, 2017) standard.

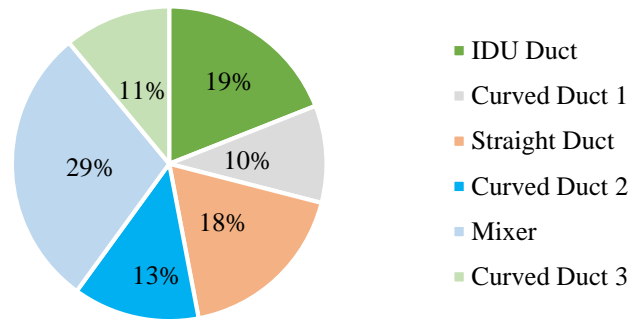


**Figure 5:** Net heat stored in code tester during cycling with heater

## 5. NEW CORRECTION METHOD

As shown earlier in Section 3, a single component may not be able to represent the thermal inertia effects of the code tester correctly. A new term defined as “thermal inertia factor (TIF)” is proposed for improving the code tester correction to the total measured capacity.  $C_d$  is measured for the same split AC system using CT-A and CT-B. TIF for both these code testers is evaluated and then an attempt is made to remove the influence of code tester on the  $C_d$ .

The TIF is defined as the ratio of integrated heat transfer to the code tester to the integrated total capacity of the tested equipment (Equation (11)). The ideal dry test cyclic cooling capacity (Equation (12)) is the cooling capacity corrected for the code tester and is an unknown. Note that Equation (12) is equivalent to the differential version of Equation (6), without ignoring the contributions of the non-dominant thermal inertia regions. If the tested equipment, i.e., capacity source, is an electric heater, it may be assumed to be instantly on and off. So the integral in the denominator of Equation (11) can be evaluated. This value is evaluated to be 6.67% for CT-A and 2.07% for CT-B when a 9 kW heater is used for the heater test described in Section 3.

$$TIF = \frac{\int_0^{t_o} \dot{Q}_{th} \cdot dt}{\int_0^{t_o} \dot{Q}_{cyc,dry,ideal} \cdot dt} \approx \frac{\int_0^{t_o} \dot{Q}_{th} \cdot dt}{\dot{Q}_{cyc,ideal} \cdot \Delta t} \quad (11)$$

$$\dot{Q}_{cyc,dry,ideal} = \dot{Q}_{cyc,dry} + \dot{Q}_{th} \quad (12)$$

When a 1.5 TR residential split AC system was subject to cyclic C and D Tests (AHRI Standard 210/240, 2017), the  $C_d$  with CT-A is 0.17 and with CT-B is 0.14. The objective of the current research is to reduce this variation arising from the variation in  $C_d$  which is assumed to be majorly from the effects of code tester thermal inertia. Equation (13) shows the equation of  $C_d$  by substituting the definitions of CLF and PLF. We can assume that the C-Test parameters are same for both systems since the thermal inertia effects are dynamic in nature. Additionally, as per Goldschmidt et al. (1980), since the cyclic power consumption has negligible degradation effect, we can assume that the work done in D-Test with both code testers is constant. This enables grouping different constants into sets  $K_1$  and  $K_2$  (Equation (14) and (15)). The ideal cooling capacity can be substituted for the measured cooling capacity. Finally, if we can substitute TIF from Equation (11), to obtain the final form shown in Equation (13) after a few algebraic manipulations. Ideal  $C_d$  can be defined as the value of  $C_d$  measured with a code tester with zero thermal inertia. Substituting  $TIF = 0$ , in Equation (13), we obtain Equation (16) for ideal  $C_d$ .

$$C_d = \frac{1 - \frac{\int_0^{t_o} (\dot{Q}_{cyc,dry}) .dt}{\dot{Q}_{ss,dry}}}{1 - \frac{\int_0^{t_o} (\dot{Q}_{cyc,dry}) .dt}{\dot{Q}_{ss} t_c}} = \frac{1 - K_1 \left( \frac{\int_0^{t_o} (\dot{Q}_{cyc,dry,ideal} - \dot{Q}_{th}) .dt}{\int_0^{t_o} (\dot{Q}_{cyc,dry,ideal} - \dot{Q}_{th}) .dt} \right)}{1 - K_2 \left( \frac{\int_0^{t_o} (\dot{Q}_{cyc,dry,ideal} - \dot{Q}_{th}) .dt}{\int_0^{t_o} (\dot{Q}_{cyc,dry,ideal} - \dot{Q}_{th}) .dt} \right)} = \frac{1 - K_1 \left( \frac{\int_0^{t_o} \dot{Q}_{cyc,dry,ideal} .dt}{\int_0^{t_o} \dot{Q}_{cyc,dry,ideal} .dt} \right) (1 - TIF)}{1 - K_2 \left( \frac{\int_0^{t_o} \dot{Q}_{cyc,dry,ideal} .dt}{\int_0^{t_o} \dot{Q}_{cyc,dry,ideal} .dt} \right) (1 - TIF)} \quad (13)$$

$$\frac{1}{K_1} = \frac{\dot{Q}_{ss,dry}}{\dot{W}_{ss,dry}} \left( \frac{\int_0^{t_o} (\dot{W}_{cyc,dry}) .dt}{\int_0^{t_o} (\dot{W}_{cyc,dry}) .dt} \right) \quad (14)$$

$$\frac{1}{K_2} = \frac{1}{\dot{Q}_{ss} t_c} \quad (15)$$

$$C_{d,ideal} = \frac{1 - K_1 \left( \frac{\int_0^{t_o} \dot{Q}_{cyc,dry,ideal} .dt}{\int_0^{t_o} \dot{Q}_{cyc,dry,ideal} .dt} \right)}{1 - K_2 \left( \frac{\int_0^{t_o} \dot{Q}_{cyc,dry,ideal} .dt}{\int_0^{t_o} \dot{Q}_{cyc,dry,ideal} .dt} \right)} \quad (16)$$

The integral in the denominator of TIF (Equation (11)) can be evaluated for the heater test with the assumption of instantaneous rise to full capacity, but not for the case of D-Test of SPAC due to the existent time delay in reaching peak capacity as a result of the refrigerant migration. For the purpose of the present discussion, the value of TIF evaluated for the heater test flow conditions is assumed to equate to the TIF during the D-Test. It is essential to understand the behavior of this term when the inlet flow conditions to the code tester are modified. Parametric study of flow conditions such as chamber temperature, heater capacity, and air flow rate to apply suitable scaling factors to the heater test TIF is part of future work. The ideal integrated cooling capacity may be evaluated from Equation (13) since measured  $C_d$ , TIF,  $K_1$  and  $K_2$  are available. Finally, Equation (16) may be used to evaluate ideal  $C_d$ . The results of these calculations are shown in Table 1. It can be observed that the ideal cooling capacity predicted is fairly close, but the evaluated ideal  $C_d$  is different. The calculation does capture qualitative trends. CT-A with higher thermal inertia needs more correction from measured  $C_d$  to ideal  $C_d$ , compared to CT-B.

**Table 1:** Evaluation of Ideal  $C_d$  for CT-A and CT-B

Code Tester	TIF [-]	$C_d$ [-]	$\int_0^{t_o} (\dot{Q}_{cyc,dry}) .dt$ [W-hr]	$\int_0^{t_o} \dot{Q}_{cyc,dry,ideal} .dt$ [W-hr]	$C_{d,ideal}$ [-]
CT-A	6.67	0.17	444.3	474.1	0.10
CT-B	2.07	0.14	461.3	471.4	0.12

The code tester model is used to conduct a parametric study of different volume flow rates and inlet air temperatures to understand the behavior of TIF. The results are shown in Figure 6. The two cases plotted are fixed volume flow rate and fixed temperature across all the heaters. These are the two variables, which determine the airflow inlet conditions to the code tester. It can be observed from the graph that the volume flow rate is the main factor affecting TIF. The heater test which is validated is at the intersection point. The thermal inertia factors are expected to lie within the boundary defined by these two extreme cases.

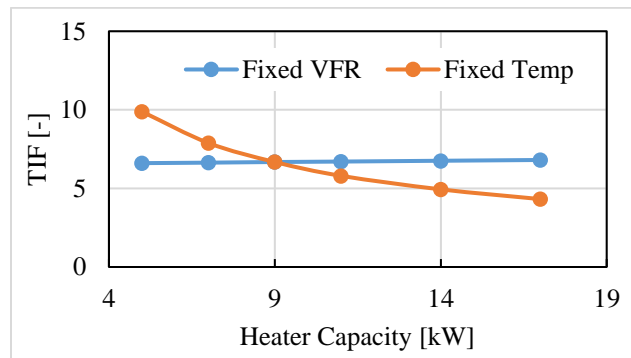


**Figure 6:** Parametric study with code tester airflow variables

One of the reasons for deviation in the ideal  $C_d$  value is that the uncertainty in the measurement of  $C_d$  itself is very high. For absolute uncertainties in pressure (1.5 Pa), RH (1%), inlet TC grid (0.6°C), outlet TC grid (0.5°C) and watt-meter (4.1 W), the relative error in the measured steady state cooling capacity = 5%, for C-Test coefficient of performance = 5%. Assuming that the relative uncertainty in D-Test cooling capacity, the coefficient of performance and work is same as that of C-Test, the total uncertainty in the measured value of  $C_d = 52\%$ ! The uncertainty propagation is carried out using the root sum square method using Engineering Equation Solver (EES). The biggest factors contributing to the uncertainty are the thermocouples on the airside.

Kapadia et al. (2009) showed that the measured cooling capacity on the refrigerant side is different from the one measured on the airside since the former does not include thermal inertia effects of code tester. Thus, using refrigerant side cooling capacity may be one way of estimating ideal  $C_d$ . Another possible reason for deviation is the value of TIF used in the calculation. The heater test operates at  $0.566 \text{ m}^3\text{s}^{-1}$  (1200 cfm), while the unit is tested at  $0.283 \text{ m}^3\text{s}^{-1}$  (600 cfm). Volume flow rate plays an important role in factoring TIF. Future work will focus on investigating the correct value of TIF for evaluating ideal  $C_d$ . Finally, the refrigerant lines connecting the IDU from ODU are of different lengths and vertical orientations. These may also have created slightly different distributions during cyclic testing and result in different  $C_d$ . The measuring equipment used has also different internal volumes, which affected the total system charge for both systems. Future work will focus on understanding contributions from all these factors to obtain a better value of  $C_d$ .

## 6. CONCLUSIONS

The present article discusses the limitations of current HVAC rating procedure and specifically targets the role of airflow measurement device contribution on the  $C_d$ . Deviations arising from assumptions used in the calculation procedure are highlighted using a validated dynamic model for the code tester. A new term called thermal inertia factor is defined and the  $C_d$  formula is modified using the thermal inertia factor to remove the impact of a specific code tester design from the measured value of  $C_d$ . Discussions on future directions aimed at improving  $C_d$  evaluation procedure is conducted.

## NOMENCLATURE

$c$	Specific heat capacity	$[\text{J kg}^{-1} \text{K}^{-1}]$	$K$	Constant group	$[\text{J}^{-1}]$
$C_d$	Cyclic degradation coefficient	$[-]$	$m$	Mass	$[\text{kg}]$
CLF	Cooling load factor	$[-]$	$q$	Integrated cooling capacity	$[\text{J}]$
$C_m$	Maximum cycling rate	$[\text{s}^{-1}]$	$\dot{Q}$	Heat transfer rate	$[\text{W}]$
COP	Coefficient of performance	$[-]$	SEER	Seasonal EER	$[\text{Btu hr}^{-1}\text{W}^{-1}]$
$C_r$	Cycling rate	$[\text{s}^{-1}]$	$t$	Time	$[\text{s}]$
EER	Energy Efficiency Ratio	$[\text{Btu hr}^{-1}\text{W}^{-1}]$	$\tau$	Time constant	$[\text{s}]$
$F_n$	Fractional on-time	$[-]$	$T$	Temperature	$[\text{K}]$
$G$	Thermal Conductance	$[\text{W/K}]$	TIF	Thermal inertia factor	$[-]$

### Subscript

B	B-Test from AHRI 210/240	on	on cycle of air conditioner
---	--------------------------	----	-----------------------------

c	complete cycle (on+off)	off	off cycle of air conditioner
cyc,dry	D-Test from AHRI 210/240	ss,dry	C-Test from AHRI 210/240
mixer	mixer	ts	thermal storage
ideal	ideal		

## REFERENCES

- AHRI Standard 210/240. (2017). Performance Rating of Unitary Air Conditioning and Air-Source Heat Pump Equipment. *Air-Conditioning, Heating, & Refrigeration Institute, Arlington, VA 22201, USA.*
- ASHRAE Standard 116. (2010). 116, Methods of Testing for Seasonal Efficiency of Unitary Air-Conditioners and Heat Pumps. *American Society of Heating, Refrigerating and Air-Conditioning Engineers, Atlanta (GA).*
- ASHRAE Standard 41.2. (1992). Standard 41.2-1987 (RA 92), Standard methods for laboratory air-flow measurement. *American Society of Heating, Refrigerating and Air-Conditioning Engineers, Inc., Atlanta.*
- Bettanini, E., Gastaldello, A., and Schibuola, L. (2003). Simplified models to simulate part load performances of air conditioning equipments. In *8th International IBPSA conference, Eindhoven, Netherland.*
- Didion, D. A., and Kelly, G. E. (1979). New testing and rating procedures for seasonal performance of heat pumps. *ASHRAE Journal, 21(9), 40–44.*
- Dittus, F. W., and Boelter, L. M. K. (1985). Heat transfer in automobile radiators of the tubular type. *International Communications in Heat and Mass Transfer, 12(1), 3–22.*
- Fuentes, E., Waddicor, D. A., and Salom, J. (2016). Improvements in the characterization of the efficiency degradation of water-to-water heat pumps under cyclic conditions. *Applied Energy, 179, 778–789.*
- Goldschmidt, V. W., Hart, G. H., and Reiner, R. C. (1980). A note on the transient performance and degradation coefficient of a field tested heat pump-cooling and heating mode. *ASHRAE Transactions, 86(Part 2), 368.*
- Henderson, H. I., Parker, D., and Huang, Y. J. (2000). Improving DOE-2's RESYS routine: User defined functions to provide more accurate part load energy use and humidity predictions. In *2000 ACEEE Summer Study on Energy Efficiency in Buildings* (p. 1.113-1.124).
- ISO Standard 16358-1. (2013). Air-cooled air conditioners and air-to-air heat pumps - testing and calculating methods for seasonal performance factors - part 1: cooling seasonal performance factor. *International Standards Organization.*
- Kapadia, R. G., Jain, S., and Agarwal, R. S. (2009). Transient characteristics of split air-conditioning systems using R-22 and R-410A as refrigerants. *HVAC&R Research, 15(3), 617–649.*
- Katipamula, S., and O'Neal, D. L. (1991). Performance degradation during on-off cycling of single-speed heat pumps operating in the cooling mode: experimental results. *ASHRAE Transactions, 97(Part 2), 331–339.*
- Kelly, G. E., and Parken Jr, W. H. (1978). Method of testing, rating and estimating the seasonal performance of central air conditioners and heat pumps operating in the cooling mode. *Final Report National Bureau of Standards, Washington, DC. Center for Building Technology.*
- Mattsson, S. E., Elmqvist, H., and Otter, M. (1998). Physical system modeling with Modelica. *Control Engineering Practice, 6(4), 501–510.*
- Mulroy, W. J., and Didion, D. (1985). Refrigerant migration in a split-unit air conditioner. *ASHRAE Transactions, 91(ASHRAE Transactions).*
- Murphy, W. E., and Goldschmidt, V. W. (1979). The degradation coefficient of a field-tested self-contained 3-ton air conditioner. *ASHRAE Transactions, 85(Part 2), 396.*
- O'Neal, D. L., and Katipamula, S. (1993). Development of nondimensional cycling model for estimating the seasonal performance of air conditioners. *Journal of Solar Energy Engineering, 115(3), 176–181.*
- Parken, W. H., Beausoliel, R. W., and Kelly, G. E. (1977). Factors affecting the Performance of a Residential Air-to-Air Heat Pump. *ASHRAE Transactions, 83(1), 839–849.*
- Schmidt, E. F. (1967). Wärmeübergang und druckverlust in rohrschlangen. *Chemie Ingenieur Technik, 39(13), 781–789.*
- Wetter, M., Zuo, W., Nouidui, T. S., and Pang, X. (2014). Modelica buildings library. *Journal of Building Performance Simulation, 7(4), 253–270.*

## ACKNOWLEDGEMENT

The authors thank the United Technologies Corporation Center of Excellence at University of Maryland for supporting this effort. The support of the members of the Center for Environmental Energy Engineering (CEEE) at University of Maryland is also acknowledged.